J|A|C|S ARTICLES

Published on Web 04/01/2010

The Influence of Spin Effects on the Gas Phase Reactions of Carbanions with N and O Atoms

Zhibo Yang,*,† Brian Eichelberger,†,|| Oscar Martinez, Jr.,† Momir Stepanovic,† Theodore P. Snow,*,‡,§ and Veronica M. Bierbaum*,†,§

Department of Chemistry and Biochemistry, Department of Astrophysical and Planetary Sciences, and Center for Astrophysics and Space Astronomy, University of Colorado, Boulder, Colorado 80309

Received January 25, 2010; E-mail: zhibo.yang@colorado.edu; tsnow@casamail.colorado.edu; veronica.bierbaum@colorado.edu

Abstract: Molecular anions have been recently detected in the denser regions of the interstellar medium. However, the chemical reactions of molecular anions with atomic species that are abundant in the ISM remain largely unexplored. This work is an experimental and computational study of CH_2CN^-, CH_3CHCN^-, $(CH_3)_2CCN^-$, and CH_2CHO^- reacting with N and O atoms. In all cases the reactions of anions with O atoms exhibit larger reaction rate constants compared to the corresponding reactions with N atoms. Our study indicates that spin-forbidden reactions are the probable pathways in the reactions with N atoms, whereas spin-allowed reactions are the dominant processes in the reactions with O atoms. The major factor influencing the reaction rate constants of anions with N and O atoms is whether a spin-allowed barrierless pathway exists. The rich chemistry observed in this work provides a greater understanding of the ion−atom reaction processes, as well as some new avenues for further spin chemistry research.

1. Introduction

Despite the harsh conditions of the interstellar medium (ISM), more than 160 molecular species have been detected in dense clouds. These compounds include a wide variety of organic functional groups and an exceptionally broad array of nitrile species. Although positive ions have been known for many years, negative ions were first detected in 2006, and the existence of five carbanions has now been confirmed in molecular clouds.[1] This exciting discovery suggests that the reactions of anions may be important in the chemical transformations and synthesis within the ISM. Because of the high abundance of N and O atoms, experiments have studied the chemistry of these atoms with organic ions in the ISM and planetary atmospheres. However, studies have focused on cations such as small hydrocarbons[2−6] and polycyclic aromatic hydrocarbons.[7−10] In contrast, little is known about the reactions of N and O atoms with organic anions.

Our recent work has investigated the reactions of carbon chain anions (C_n^- and HC_n^-) with atomic species, i.e, $N(^4S)$ and $O(^3P)$, which may pose intriguing questions of spin conservation and spin conversion.[11] In chemical reactions, the conservation of the total electron spin is a fundamental and universal principle, whereas conversion of spin is required for spin-forbidden reactions. It is well-known that in many cases spin chemistry may play an important role in determining the reaction mechanisms and rate constants of ion−atom reactions.[10,12−23] Except

† Department of Chemistry and Biochemistry.
‡ Department of Astrophysical and Planetary Sciences.
§ Center for Astrophysics and Space Astronomy.
|| Current address: Department of Chemistry, John Brown University, Siloam Spring, Arkansas 72761.

(1) (a) McCarthy, M. C.; Gottlieb, C. A.; Gupta, H.; Thaddeus, P. *Astrophys. J.* **2006**, *652*, L141–L144. (b) Cernicharo, J.; Guélin, M.; Agúndez, M.; Kawaguchi, K.; McCarthy, M.; Thaddeus, P. *Astron. Astrophys.* **2007**, *467*, L37–L40. (c) Brünken, S.; Gupta, H.; Gottlieb, C. A.; McCarthy, M. C.; Thaddeus, P. *Astrophys. J.* **2007**, *664*, L43–L46. (d) Remijan, A. J.; Hollis, J. M.; Lovas, F. J.; Cordiner, M. A.; Millar, T. J.; Markwick-Kemper, A. J.; Jewell, P. R. *Astrophys. J.* **2007**, *664*, L47–L50. (e) Thaddeus, P.; Gottlieb, C. A.; Gupta, H.; Brünken, S.; McCarthy, M. C.; Agúndez, M.; Guélin, M.; Cernicharo, J. *Astrophys. J.* **2008**, *677*, 1132–1139. (f) Cernicharo, J.; Guélin, M.; Agú, M.; McCarthy, M. C.; Thaddeus, P. *Astrophys. J.* **2008**, *688*, L83–L86.
(2) McEwan, M. J.; Scott, G. B. I.; Adams, N. G.; Babcock, L. M.; Terzieva, R.; Herbst, E. *Astrophys. J.* **1999**, *513*, 287–293.
(3) Scott, G. B. I.; Fairley, D. A.; Freeman, C. G.; McEwan, M. J.; Anicich, V. G. *J. Chem. Phys.* **1998**, *109*, 9010–9014.
(4) Scott, G. B. I.; Fairley, D. A.; Freeman, C. G.; McEwan, M. J.; Anicich, V. G. *J. Phys. Chem. A* **1999**, *103*, 1073–1077.
(5) Scott, G. B. I.; Fairley, D. A.; Milligan, D. B.; Freeman, C. G.; McEwan, M. J. *J. Phys. Chem. A* **1999**, *103*, 7470–7473.
(6) Scott, G. B. I.; Milligan, D. B.; Fairley, D. A.; Freeman, C. G.; McEwan, M. J. *J. Chem. Phys.* **2000**, *112*, 4959–4965.
(7) Le Page, V.; Keheyan, Y.; Bierbaum, V. M.; Snow, T. P. *J. Am. Chem. Soc.* **1997**, *119*, 8373–8374.
(8) Snow, T. P.; Le Page, V.; Keheyan, Y.; Bierbaum, V. M. *Nature* **1998**, *391*, 259–260.
(9) Le Page, V.; Keheyan, Y.; Snow, T. P.; Bierbaum, V. M. *J. Am. Chem. Soc.* **1999**, *121*, 9435–9446.
(10) Le Page, V.; Keheyan, Y.; Snow, T. P.; Bierbaum, V. M. *Int. J. Mass Spectrom.* **1999**, *185/186/187*, 949–959.
(11) Eichelberger, B.; Snow, T. P.; Barckholtz, C.; Bierbaum, V. M. *Astrophys. J.* **2007**, *667*, 1283–1289.
(12) Schwarz, H. *Int. J. Mass Spectrom.* **2004**, *237*, 75–105.
(13) Sablier, M.; Rolando, C. *Mass Spectrom. Rev.* **1993**, *12*, 285–312.
(14) Goldan, P. D.; Schmeltekopf, A. L.; Fehsenfeld, F. C.; Schiff, H. I.; Ferguson, E. E. *J. Chem. Phys.* **1966**, *44*, 4095–4103.
(15) Ferguson, E. E.; Fehsenfeld, F. C.; Schmeltekopf, A. L. *Adv. At. Mol. Phys.* **1969**, *5*, 1–56.
(16) Ferguson, E. E. *Chem. Phys. Lett.* **1983**, *99*, 89–92.
(17) Federer, W.; Villinger, H.; Lindinger, W.; Ferguson, E. E. *Chem. Phys. Lett.* **1986**, *123*, 12–16.
(18) Stowe, G. F.; Schultz, R. H.; Wight, C. A.; Armentrout, P. B. *Int. J. Mass Spectrom. Ion Processes* **1990**, *100*, 177–195.

 10.1021/ja100673z

for a few cases, the spin-allowed exothermic ion−molecule reactions are generally much faster than the corresponding spin-forbidden reactions, and this has been attributed to weak spin−orbital coupling, *i.e.*, slow spin conversion between different spin states in the spin-forbidden reactions.[12,17] In addition to the influence on the reactivity and mechanism, electron spin has recently been found to be crucial in other studies including the properties of nanoparticles,[24] molecular conductors,[25] hydrogen storage materials,[26] information storage materials,[27] *etc*.

Regarding reaction kinetics, experimental studies have shown that $O(^3P)$ is more reactive than $N(^4S)$ in reactions with ions.[11,28] The significant difference in the electron affinity for N (<0)[29] and O (1.46 eV)[30] atoms may contribute to the higher reactivity of O atoms with anions. However, this explanation is not applicable to the reactions of cations with N and O atoms, where the reactions between cations and N atoms are also generally slower than the corresponding reactions with O atoms. Therefore, more studies are needed to understand the factors affecting reaction rate constants of ion−atom reactions.

Published computational results[23] have shown that the reaction between cyclic $C_3H_3^+$ (closed-shell) and ground state $N(^4S)$ atoms is totally prohibited due to the repulsive potential energy surface; this has been attributed to the dominance of electron−electron repulsion regardless of the ion−neutral attraction between the two species. This result suggests that the nature of the potential energy surface along the approach of the ions and atoms may be a crucial factor in determining the difference in reaction rate constants for spin-allowed and spin-forbidden reactions.

The present study details the chemistry of three nitrile anions (CH_2CN^-, CH_3CHCN^-, $(CH_3)_2CCN^-$) and a prototypical aldehyde (CH_2CHO^-) with N and O atoms to explore general reactivity and determine reaction pathways. Computational studies allow us to characterize the energies of the reactants, ion complexes, transition states, and products as well as to probe the applicability of spin conservation rules in ion−atom reactions.

2. Experimental Methods

Measurements of the reaction rate coefficients and product distributions were made using the tandem flowing afterglow-selected ion flow tube (FA-SIFT) at the University of Colorado, Boulder. This instrument has been described elsewhere,[31] and only the salient details for these experiments will be discussed here.

Ions were generated using electron impact and chemical ionization methods in the source flow tube. A small flow of N_2O entrained in helium buffer gas was passed over a rhenium filament to generate O^-, which further reacted with CH_4 to form OH^-. The desired organic anion was then produced by reaction of OH^- with the corresponding neutral precursor, HA:

$$OH^- + HA \rightarrow H_2O + A^-$$

The organic anion was mass-selected with the SIFT quadrupole mass filter and injected into the reaction flow tube through a venturi inlet. The ions were entrained in helium buffer gas (0.4 Torr, 200 std cm^3 s^{-1}) at 298 K and relaxed by multiple collisions. The ion−neutral reaction was initiated by adding N or O atoms to the flow tube through an inlet positioned 70 cm upstream of the sampling orifice. Reactant and product ions were monitored with a quadrupole mass filter coupled with an electron multiplier.

Microwave discharge techniques were used to generate N and O atoms in their ground states. This is a well-established method that is amenable to the study of the reactions of ions with atoms using an FA-SIFT.[4−8,10,11] The N atoms were generated by flowing N_2 through a microwave discharge cavity operating at 30−60 W; vibrationally excited N_2 molecules formed in the discharge are not expected to be reactive.[32] The $O(^3P)$ atoms were formed by the subsequent titration of the N atoms with NO (5% NO in He) according to the reaction $N(^4S) + NO \rightarrow N_2 + O(^3P)$. Because of difficulties in measuring the absolute number densities of atoms, the total error in the rate constant measurements is estimated as ±50%.

3. Theoretical Calculations

To obtain the structures and energies of the anions and neutral species involved in the current study, theoretical calculations were carried out using the Gaussian 03 suite of programs.[33] Geometry optimization and frequency analyses were calculated at the MP2(full)/aug-cc-pVDZ level of theory. Zero-point energy (ZPE) and thermal energy (298 K) corrections were included at the same level of theory. Unless otherwise noted, the single-point energy was calculated at the (RO)MP2(full)/aug-cc-pVTZ level of theory for the optimized structures, where the restricted open-shell method (ROMP2(full)) was applied to the open-shell species to minimize the influence of spin contamination on the energies, and the basis set superposition error (BSSE) correction was also included at this level of theory. The computational results were used to construct the reaction coordinate plots of four selected systems and to calculate the enthalpies of all reactions involved in the current study. The crossing points between the potential energy surfaces of

(19) Rue, C.; Armentrout, P. B.; Kretzschmar, I.; Schröder, D.; Harvey, J. N.; Schwarz, H. *J. Chem. Phys.* **1999**, *110*, 7858–7870.
(20) Huang, X.; Xing, G.; Bersohn, R. *J. Chem. Phys.* **1994**, *101*, 5818–5823.
(21) Xing, G.; Huang, X.; Wang, X. B.; Bersohn, R. *J. Chem. Phys.* **1996**, *105*, 488–495.
(22) Yarkony, D. R. *J. Phys. Chem. A* **1998**, *102*, 5305–5311.
(23) Takagi, N.; Fukuzawa, K.; Osamura, Y.; Schaefer, H. F. *Astrophys. J.* **1999**, *525*, 791–798.
(24) (a) Zhu, K.; Hu, J.; She, X.; Liu, J.; Nie, Z.; Wang, Y.; Peden, C. H. F.; Kwak, J. H. *J. Am. Chem. Soc.* **2009**, *131*, 9715–9721. (b) Hsia, C. H.; Chen, T. Y.; Son, D. H. *J. Am. Chem. Soc.* **2009**, *131*, 9146–9147.
(25) (a) Takahashi, K.; Cui, H. B.; Okano, Y.; Kobayashi, H.; Mori, H.; Tajima, H.; Einaga, Y.; Sato, O. *J. Am. Chem. Soc.* **2008**, *130*, 6688–6689. (b) Djukic, B.; Lemaire, M. T. *Inorg. Chem.* **2009**, *48*, 10489–10491. (c) Huang, J.; Kertesz, M. *J. Am. Chem. Soc.* **2003**, *125*, 13334–13335.
(26) (a) Halder, G. J.; Kepert, C. J.; Moubaraki, B.; Murray, K. S.; Cashion, J. D. *Science* **2002**, *298*, 1762–1765. (b) Horike, S.; Shimomura, S.; Kitagawa, S. *Nat. Chem.* **2009**, *1*, 695–704. (c) Liu, J. J.; Ge, Q. F. *J. Chem. Theory Comput.* **2009**, *5*, 3079–3087.
(27) (a) Fujisawa, T.; Austing, D. G.; Tokura, Y.; Hirayama, Y.; Tarucha, S. *Nature* **2002**, *419*, 278–281. (b) Bandyopadhyay, S.; Cahay, M. *Nanotechnology* **2009**, *20*, 412001. (c) Chappert, C.; Fert, A.; Van Dau, F. N. *Nat. Mater.* **2007**, *6*, 813–823.
(28) Snow, T. P.; Bierbaum, V. M. *Annu. Rev. Anal. Chem.* **2008**, *1*, 229–259.
(29) Brown, T. L.; LeMay, H. E., Jr.; Bursten, B. E. *Chemistry, The Central Science*, 8th ed.; Prentice-Hall, Inc.: Upper Saddle River, NJ, 2000; p 237. Electron affinity < 0 indicates that the negative ion is higher in energy than the separated atom and electron.
(30) (a) Linstrom, P. J., Mallard, W. G., Eds. *NIST Chemistry WebBook, NIST Standard Reference Database Number 69*; National Institute of Standards and Technology: Gaithersburg, MD, 20899, http://webbook.nist.gov (retrieved November 3, 2009). (b) Valli, C.; Blondel, C.; Delsart, C. *Phys. Rev. A* **1999**, *59*, 3809–3815.
(31) Van Doren, J. M.; Barlow, S. E.; DePuy, C. H.; Bierbaum, V. M. *Int. J. Mass Spectrom. Ion Processes* **1987**, *81*, 85–100.
(32) (a) Clynne, M. A. A.; Nip, W. S. In *Reactive Intermediates in the Gas Phase*; Setser, D. W., Ed.; Academic Press: New York, NY, 1979; p 12. (b) Evans, H. G.; Winkler, C. A. V. *Can. J. Chem.* **1956**, *34*, 1217–1231. (c) Kaufman, F.; Kelso, J. R. *J. Chem. Phys.* **1958**, *28*, 510–511.
(33) Frisch, M. J. et al. *Gaussian 03*; Gaussian, Inc.: Wallingford, CT, 2004.

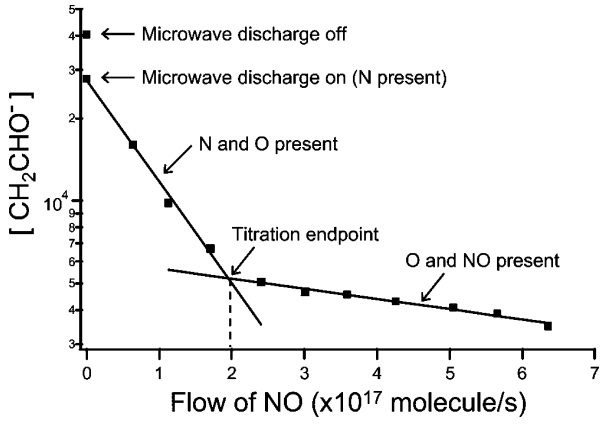

Figure 1. Titration plot for the reaction of CH_2CHO^- with N and O.

different spin states were explored using the program developed by Harvey et al.[34]

4. Results and Discussion

The reactant ions CH_2CN^-, CH_3CHCN^-, $(CH_3)_2CCN^-$, and CH_2CHO^- were allowed to react with N and O atoms. Figure 1 shows a typical titration plot, where the logarithm of the intensity of CH_2CHO^- is plotted versus the flow of NO. The higher point on the *y*-axis, for which the flow of NO is zero, corresponds to conditions where molecular nitrogen is flowing into the system, but the microwave discharge is off; no reaction is evident. When the discharge is ignited, N atoms are formed, the ions react, and their intensity decreases to the lower value on the *y*-axis. As NO is added to the system, N is converted to O, and the ion signal decreases due to the more rapid reaction of CH_2CHO^- with O. The intersection of the two lines represents the end point of the titration; the flow of NO at this point is both the N atom flow at the beginning of the titration as well as the O atom flow at the end point. Further addition of NO beyond the end point causes only a slight decrease in ion signal. The reaction rate constants are determined from the ion loss, the atom flow rate, and other experimental parameters.

The rate constants and products for reactions of the carbanions with N and O atoms are summarized in Table 1. Reaction efficiencies are reported with respect to k_{PPI}, a point-polarizable-ion adjustment to traditional Langevin theory as detailed elsewhere; the approach includes the polarizability of the carbanion in the calculation of the collision rate constant.[35] The only observable ionic product for the reactions with N atoms is CN^-. Similarly, for the reactions with O atoms, CN^- is the dominant ionic product in all reactions, whereas CCN^- was also detected in the reaction of CH_2CN^- + O. The rate constants and efficiencies for reactions with O atoms are higher than the corresponding reactions with N atoms. Although there are multiple possibilities for the neutral products in each case, the neutral species are not detected in our experiments.

4.1. Reactions of CH_2CN^-, CH_3CHCN^-, and $(CH_3)_2CCN^-$ with N Atoms. The reactions of anions with N atoms and O atoms can occur by multiple channels. Theoretical calculations were carried out to investigate the reaction mechanisms proposed, and results are shown on the reaction coordinate plots (Figures 2, 4, 5, and 7), where all energies are relative to the corresponding reactants in each of the four selected systems. The enthalpies of the possible reaction channels were calculated as summarized in Table 1.

As the first example, the reaction coordinate plot of CH_2CN^- + N is shown in Figure 2, where the energy landscapes of all possible reactions are indicated. The spin-conserved reaction pathway has an energy barrier along the approach of the reactants, and the only exothermic channel is associative detachment to form neutral NCH_2CN (triplet), which is 18.5 kcal/mol below the total energy of reactants.

$$^-CH_2CN\ (S) + N\ (Q) \rightarrow NCH_2CN\ (T) + e^-, \quad \Delta H_0 = -18.5\ \text{kcal/mol} \qquad (1)$$

For this example and all subsequent discussion, the parenthetical letter after the chemical formula indicates the spin state, i.e., singlet (S), doublet (D), triplet (T), or quartet (Q). According to our calculations carried out at the (RO)MP2(full)/aug-cc-pVTZ//MP2(full)/aug-cc-pVDZ level of theory, the height of this energy barrier is 11.5 kcal/mol, whereas a lower energy barrier (7.8 kcal/mol) was obtained using the CCSD(T)/aug-cc-pVTZ//MP2(full)/aug-cc-pVDZ level of theory. This energy barrier cannot be overcome by the reactants, such that the spin-conserved reaction is not feasible.

The only ionic product observed in the experiment is CN^-. Our calculations indicate that the singlet state of CN^- is more stable than the triplet state by 168.4 kcal/mol, and the corresponding neutral counterpart fragment, CH_2N, has a doublet ground state that is more stable than its quartet state by 90.4 kcal/mol. Thus, reactions to produce these spin conserved products, i.e., CN^- (S) + CH_2N (Q) or CN^- (T) + CH_2N (D), are endothermic processes by 36.6 or 114.6 kcal/mol, respectively; these processes cannot occur under the experimental conditions. These results indicate that the products must be CN^- (S) + CH_2N (D), which have a different total spin relative to the reactants; therefore, spin conversion from the quartet state to the doublet state must have occurred during the reaction:

$$^-CH_2CN\ (S) + N\ (Q) \rightarrow {}^-CN\ (S) + H_2CN\ (D), \quad \Delta H_0 = -53.8\ \text{kcal/mol} \qquad (2)$$

Because spin conversion is involved in this reaction, other spin-forbidden reaction pathways must be considered. One of them is a reactive detachment channel, which produces two closed shell nitriles and an electron through multiple steps:

$$^-CH_2CN\ (S) + N\ (Q) \rightarrow 2\ HCN\ (S) + e^-, \quad \Delta H_0 = -80.0\ \text{kcal/mol} \qquad (3)$$

Another possible spin-forbidden reaction pathway is an electron detachment process, in which the initial association of $^-CH_2CN$ and N forms the doublet NCH_2CN^-; hydrogen atom transfer from carbon to nitrogen then forms an isomeric species that can eject an electron. The formation of singlet HNCHCN is calculated to be exothermic by 78.6 kcal/mol (Table 1).

$$^-CH_2CN\ (S) + N\ (Q) \rightarrow HNCHCN\ (S) + e^-, \quad \Delta H_0 = -78.6\ \text{kcal/mol} \qquad (4)$$

(34) (a) Harvey, J. N.; Aschi, M.; Schwarz, H.; Koch, W. *Theor. Chem. Acc.* **1998**, *99*, 95–99. (b) Harvey, J. N.; Aschi, M. *Phys. Chem. Chem. Phys.* **1999**, *1*, 5555–5563. (c) Poli, R.; Harvey, J. N. *Chem. Soc. Rev.* **2003**, *32*, 1–8. (d) Harvey, J. N. *Phys. Chem. Chem. Phys.* **2007**, *9*, 331–343.

(35) Eichelberger, B. R.; Snow, T. P.; Bierbaum, V. M. *J. Am. Soc. Mass Spectrom.* **2003**, *14*, 501–505.

Table 1. Reactions of Carbanions with N (Q) and O (T) Atoms

Reaction[a]	Spin-allowed	Barrierless	ΔH_0[b] (kcal/mol)	ΔH_{298}[c] (kcal/mol)	k_{exp}[d] (10^{-10}cm^3/s)	Efficiency[e] (k_{exp}/k_{PPI})
$CH_2CN^- + N \rightarrow NCH_2CN$ (T) + e^-	Y	N	-18.5	-18.2	0.36 ± 0.14	0.04
$\rightarrow$ **CN^-** + H_2CN (D)	N	Y	-53.8	-52.2		
$\rightarrow$ 2HCN + e^-	N	Y	-80.0	-78.5		
$\rightarrow$ HNCHCN + e^-	N	Y	-78.6	-78.4		
$CH_3CHCN^- + N \rightarrow CH_3CH(N)CN$ (T) + e^-	Y	N	-22.5	-22.1	0.64 ± 0.13	0.08
$\rightarrow$ **CN^-** + CH_3CHN (D)	N	Y	-67.2	-65.8		
$(CH_3)_2CCN^- + N \rightarrow (CH_3)_2C(N)CN$ (T) + e^-	Y	N	-26.2	-25.5	0.15 ± 0.02	0.02
$\rightarrow$ **CN^-** + $(CH_3)_2CN$ (D)	N	Y	-71.4	-69.6		
$CH_2CHO^- + N \rightarrow NCH_2CHO$ (T) + e^-	Y	N	-13.9	-13.3	0.32 ± 0.09	0.04
$\rightarrow$ CN^- + CH_2OH (D)	N	Y	-63.2	-60.6		
$\rightarrow$ CH_2O + HCN + e^-	N	Y	-70.6	-68.7		
$CH_2CN^- + O \rightarrow$ **CN^-** + CH_2O (T)	Y	Y	-18.7	-17.0	8.5 ± 0.3	1.2
$\rightarrow$ **CCN^-** (T) + H_2O	Y	Y	-43.7	-41.9		
$\rightarrow$ OCH_2CN (D) + e^-	Y	Y	-37.1	-36.8		
$\rightarrow$ **CN^-** + CH_2O	N	Y	-97.9	-96.4		
$\rightarrow$ **CCN^-** + H_2O	N	Y	-20.6	-18.7		
$CH_3CHCN^- + O \rightarrow$ **CN^-** + CH_3CHO (T)	Y	Y	-22.5	-21.0	7.2 ± 0.2	1.0
$\rightarrow$ $CH_3CH(O)CN$ (D) + e^-	Y	Y	-44.3	-43.9		
$\rightarrow$ **CN^-** + CH_3CHO	N	Y	-109.4	-109.3		
$(CH_3)_2CCN^- + O \rightarrow$ **CN^-** + $(CH_3)_2CO$ (T)	Y	Y	-26.1	-24.2	7.7 ± 0.3	1.1
$\rightarrow$ $(CH_3)_2C(O)CN$ (D) + e^-	Y	Y	-48.7	-47.9		
$\rightarrow$ **CN^-** + $(CH_3)_2CO$	N	Y	-116.0	-114.0		
$CH_2CHO^- + O \rightarrow OCH_2CHO$ (D) + e^-	Y	Y	-36.3	-35.6	7.0 ± 0.3	0.98
$\rightarrow$ $OCCH_2OH$ (D) + e^-	N[f]	Y	-58.3	-57.5		
$\rightarrow$ CH_2O + HCO^-	N	Y	-44.2	-42.2		
$\rightarrow$ CH_3O^- + CO	N	Y	-82.9	-81.2		

[a] The reactant anions are singlets. The parenthetical letter after the chemical formula indicates the spin state of the species, *i.e.*, singlet (S), doublet (D), triplet (T), and quartet (Q). Unless noted otherwise, the molecular products are singlet states. Product ions observed in the experiment are in bold font, whereas their branching ratios were not measured due to the difficulty of evaluating the associative detachment channel. [b] Calculated at the (RO)MP2(full)/aug-cc-pVTZ//MP2(full)/aug-cc-pVDZ level of theory including zero-point energy corrections and basis set superposition error (BSSE) corrections. [c] Thermal energy (298.15 K) and BSSE corrections are included. [d] Reported error bars represent one standard deviation of the measurements. The total error is estimated as ±50%. [e] k_{PPI} is the theoretical collision rate constant obtained from the point-polarizable-ion model.[35] [f] Arises from a singlet reaction pathway which involves spin conversion.

Although reactions 3 and 4 are more exothermic than reaction 2, CN^- elimination by reaction 2 has the lowest energy barrier (−24.8 kcal/mol) among the spin-forbidden reaction pathways, indicating that production of CN^- is the preferred channel. These computational results are consistent with the experimental results that CN^- is the major product.

To investigate the crossing point between the doublet and quartet states, the relaxed potential energy scans of both spin states performed at the B3LYP/6-31+G(d,p) level of theory are shown in Figure 3. More accurate searching for the crossing point was performed at the same level of theory using the program developed by Harvey et al.,[34] and the results are also shown in Figure 3. The results indicate that the ground state reactants are on an attractive potential energy surface (quartet state) at long distances (N−C bond length > 2.634 Å) due to the charge-induced dipole interaction; however, closer approach results in repulsion between the reactants, such that curve crossing occurs between the two states. The results indicate that the N−C bond length at the crossing point is ∼2.187 Å; this value is longer than the corresponding bond length (1.786 Å) in the transition state that precedes the formation of the anion−N atom associative intermediate. In addition, the crossing point is slightly above the total energy of the reactants by 0.5 kcal/mol; this result is sufficient to give the qualitatively correct trend that the process from the reactants to the crossing point is nearly thermoneutral. Under the experimental conditions, the reactants have a thermal distribution of kinetic and internal energies, such that some reactants possess more energy than this barrier height; therefore, it might be expected that the reaction efficiency should be higher than the experimental result (0.04). However, spin-forbidden reactions are generally slower than the analogous spin-conserved processes by 1 to 4 orders of magnitude determined by the spin−orbit coupling strength.[34d] Therefore, only a small portion of reactants may possess sufficient energy to pass through the crossing point and initiate spin conversion with a measurable rate.

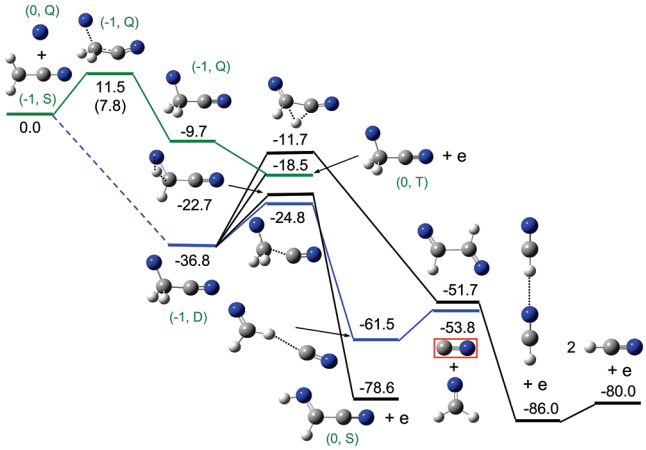

Figure 2. Reaction coordinate plot for $CH_2CN^- + N$ at 0 K. Calculations were performed at the (RO)MP2(full)/aug-cc-pVTZ//MP2(full)/aug-cc-pVDZ level of theory, and the energy value in parentheses was obtained from the CCSD(T)/aug-cc-pVTZ//MP2(full)/aug-cc-pVDZ level of theory as described in the text. The number and letter in the parentheses indicate the charge and multiplicity for each state, respectively. The spin-allowed reaction is shown as the green line, the most dynamically favorable spin-forbidden channel is shown as the blue line, and other possible reaction channels are shown as black lines. The spin-conversion process is shown as a dashed line. The observed ionic product is indicated in the red box.

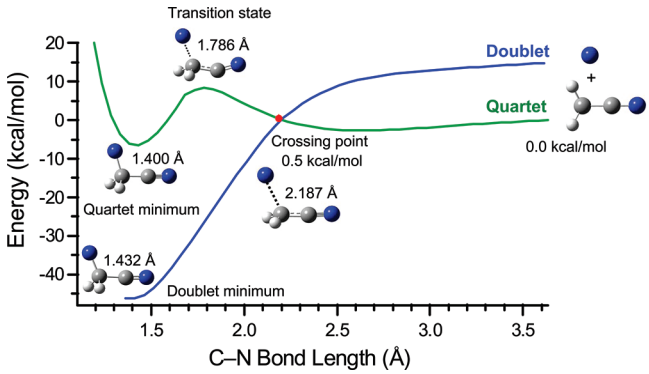

Figure 3. Relaxed potential energy surface scan of the entrance channel of $CH_2CN^- + N(^4S)$ for doublet and quartet spin states. The doublet-quartet crossing point was located using the program developed by Harvey et al.[34] shown as the red spot. All the calculations were performed at the B3LYP/6-31+G(d,P) level of theory.

Due to limited computational resources, the complete reaction coordinate plots for the reactions between N atoms and the larger nitrile anions, i.e., CH_3CHCN^- and $(CH_3)_2CCN^-$, were not constructed. Instead, only the enthalpies of the ion complexes corresponding to reactive detachment (reaction 1) and CN^- generation (reaction 2) were calculated as summarized in Table 1. In general, these reaction pathways are more exothermic than the corresponding channels in the $CH_2CN^- + N$ system. It is noted that both systems have very low reaction efficiencies, with 0.08 and 0.02 for CH_3CHCN^- and $(CH_3)_2CCN^-$ (Table 1), respectively. Because CN^- is the only ionic product, it is likely that the total spin of the products is a doublet and that spin conversion has occurred during the reactions.

4.2. Reaction of CH_2CHO^- with N Atoms. As the second computational example, the reaction coordinate plot of $CH_2CHO^- + N$ is shown in Figure 4. Because ionic products were not detected in this reaction, only electron detachment processes occur. Similar to the reaction of CH_2CN^- with N atoms, the spin-conserved reaction pathway has an energy barrier

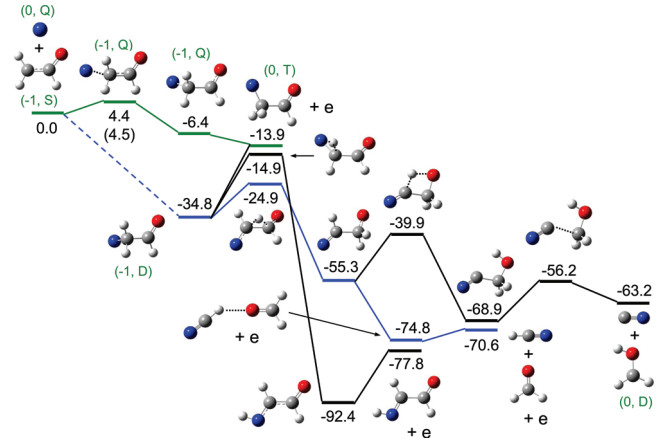

Figure 4. Reaction coordinate plot for $CH_2CHO^- + N$ at 0 K. Calculations were performed at the (RO)MP2(full)/aug-cc-pVTZ//MP2(full)/aug-cc-pVDZ level of theory, and the value in the parentheses was obtained from CCSD(T)/aug-cc-pVTZ//MP2(full)/aug-cc-pVDZ as described in the text. The number and letter in the parentheses indicate the charge and multiplicity for each state, respectively. The spin-allowed reaction is shown as the green line, the most dynamically favorable spin-forbidden channel is shown as the blue line, and other possible reaction channels are shown as black lines. The spin-conversion process is shown as a dashed line. No ionic product is observed.

along the approach of reactants, and the only possible product is the neutral triplet from electron detachment.

$$^-CH_2CHO\ (S) + N\ (Q) \rightarrow NCH_2CHO\ (T) + e^-, \quad \Delta H_0 = -13.9\ \text{kcal/mol} \qquad (5)$$

The energy barrier was obtained as 4.4 or 4.5 kcal/mol according to our calculations at the ROMP2(full)/aug-cc-pVTZ//MP2(full)/aug-cc-pVDZ or CCSD(T)/aug-cc-pVTZ//MP2(full)/aug-cc-pVDZ levels of theory, respectively, indicating that the spin-conserved reaction is not likely to occur for thermal energy reactants.

The search results for the doublet-quartet crossing point (not shown) indicate that the energy of the crossing point is close to the total energy of the reactants, such that it is possible that spin conversion occurs during the reaction, and the energetically accessible spin forbidden reactions are

$$^-CH_2CHO\ (S) + N\ (Q) \rightarrow HCN\ (S) + CH_2O\ (S) + e^-, \quad \Delta H_0 = -70.6\ \text{kcal/mol} \qquad (6)$$

$$^-CH_2CHO\ (S) + N\ (Q) \rightarrow {}^-CN\ (S) + CH_2OH\ (D), \quad \Delta H_0 = -63.2\ \text{kcal/mol} \qquad (7)$$

The most favored pathway is reaction 6 due to the presence of the lowest energy barrier (−24.9 kcal/mol). Although it is plausible that other electron detachment reactions are energetically accessible, they have higher energy barriers and are less favored channels compared to reaction 6. In addition, these reactions lead to neutral molecules that cannot be confirmed from the experimental observations. This explanation is consistent with the experimental results that an ionic product was not detected in the reaction of $CH_2CHO^- + N$. Similarly, the low reaction efficiency (0.04) is attributed to the low spin conversion efficiency at the crossing point, which has similar energy as the reactants on the entrance channel.

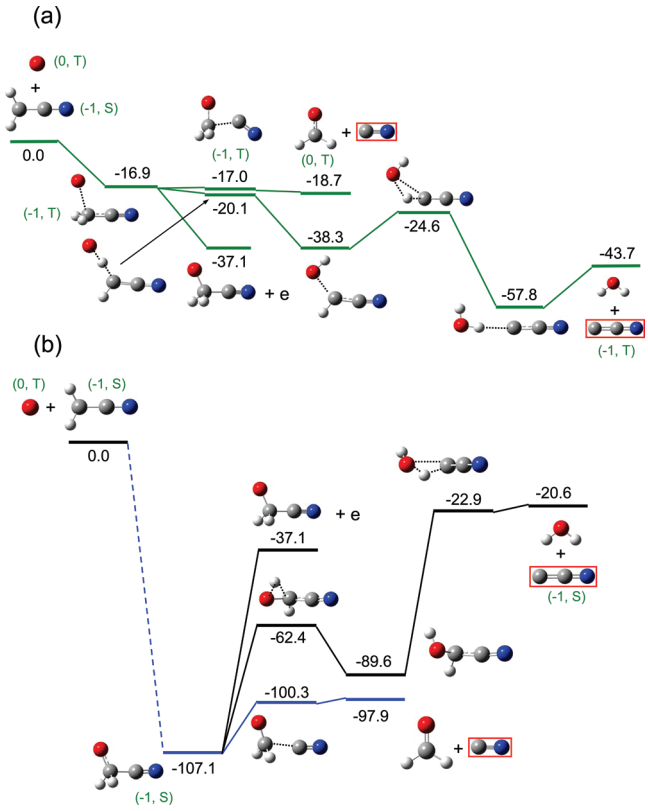

Figure 5. The reaction coordinate plot for CH_2CN^- + O of (a) spin-allowed and (b) spin-forbidden reactions at 0 K. Calculations were performed at the (RO)MP2(full)/aug-cc-pVTZ//MP2(full)/aug-cc-pVDZ level of theory as described in the text. The number and letter in the parentheses indicate the charge and multiplicity for each state, respectively. The spin-allowed reaction is shown as the green line, the most dynamically favorable spin-forbidden channel is shown as the blue line, and other possible reaction channels are shown as black lines. The spin-conversion process is shown as a dashed line. The observed product ions are indicated in the red boxes.

4.3. Reactions of CH_2CN^-, CH_3CHCN^-, and $(CH_3)_2CCN^-$ with O Atoms. The reaction coordinate plot for CH_2CN^- + O is shown in Figure 5a and b as the third example. Unlike the reaction of CH_2CN^- with N atoms, there is no energy barrier along the approach of the reactants, and the reaction efficiency is very high (~1.0), indicating that this reaction is essentially collision controlled. The three possible spin-conserved reaction channels are shown in Figure 5a. The first pathway is the formation of the neutral OCH_2CN (doublet) from the triplet intermediate through an electron detachment process, in which the O atom attaches and an electron is ejected without further rearrangement:

$$^-CH_2CN\ (S) + O\ (T) \rightarrow OCH_2CN\ (D) + e^-, \quad \Delta H_0 = -37.1\ \text{kcal/mol} \qquad (8)$$

The other pathways are the generation of CN^- and CCN^-. The direct association of CH_2CN^- with O atoms forms the triplet intermediate (−16.9 kcal/mol), which can either directly dissociate into CH_2O and CN^- (reaction 9) *via* C−C bond cleavage or form H_2O and CCN^- through two other transition states and two intermediates (reaction 10). The generation of CN^- is a simple addition−elimination mechanism:

$$^-CH_2CN\ (S) + O\ (T) \rightarrow {}^-CN\ (S) + CH_2O\ (T), \quad \Delta H_0 = -18.7\ \text{kcal/mol} \qquad (9)$$

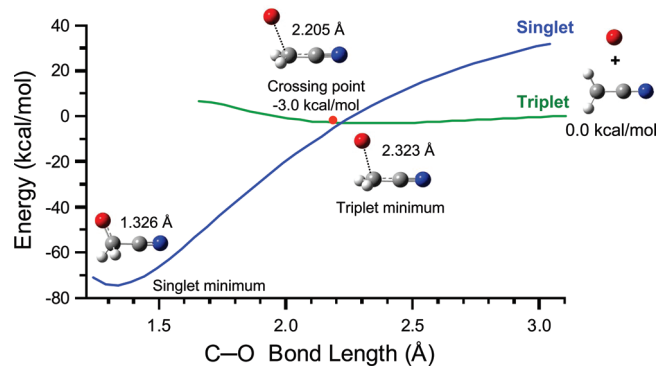

Figure 6. Relaxed potential energy surface scan of the entrance channel of CH_2CN^- + $O(^3P)$ for singlet and triplet spin states. The singlet−triplet crossing point was located using the program developed by Harvey et al.[34] shown as the red spot. All the calculations were performed at the B3LYP/6-31+G(d,P) level of theory.

In this process, the O atom adds in much the same way as the N atom adds in reaction 2, and CN^- is generated along with triplet CH_2O, which is less stable than its singlet state by 79.0 kcal/mol.

Triplet CCN^- is more stable than its singlet state by 25.4 kcal/mol, and its generation requires a more complex mechanism in which both hydrogen atoms transfer to oxygen:

$$^-CH_2CN\ (S) + O\ (T) \rightarrow {}^-CCN\ (T) + H_2O\ (S), \quad \Delta H_0 = -43.7\ \text{kcal/mol} \qquad (10)$$

According to the calculated reaction coordinate plot, reactions proceeding through all the spin-conserved pathways are energetically accessible. The direct electron detachment from the triplet intermediate forms the neutral product that is 37.1 kcal/mol below the total energy of the reactants, such that this reaction channel is also likely to occur, although the neutral product cannot be observed under our experimental conditions. Because reactions 9 and 10 have very similar energy barrier heights, the major ionic products of this reaction are expected to be CN^- and CCN^- with similar abundance, which is consistent with the experimental results.

Calculations indicate that the relative energy of the singlet−triplet crossing point is very close to the minimum structure of the triplet state on the attractive potential energy curve as shown in Figure 6, such that spin conversion may occur with measurable efficiency during the reaction of CH_2CN^- with O atoms. The possible spin-forbidden reaction pathways were investigated and shown in Figure 5b. The first pathway is the formation of the neutral OCH_2CN (doublet, −37.1 kcal/mol) from the singlet intermediate by an electron detachment process; the second pathway is the production of CN^-, and the total energy of the products is 97.9 kcal/mol below the reactants; the third pathway is CCN^- (singlet) production channel, and the products are 20.6 kcal/mol below the reactants. The CN^- producing pathway is the lowest energy pathway among the three reaction channels, *i.e.*, the most favored spin-forbidden reaction channel, and it may have a pronounced contribution to the total CN^- production if spin-forbidden reactions can compete with spin-allowed reactions. However, the spin-allowed reactions presumably result in the production of similarly abundant CN^- and CCN^- as is observed experimentally, suggesting that CN^- is mainly produced from the spin-allowed pathway. Therefore, the spin-forbidden channels do not appear to compete with spin-allowed pathways in this reaction.

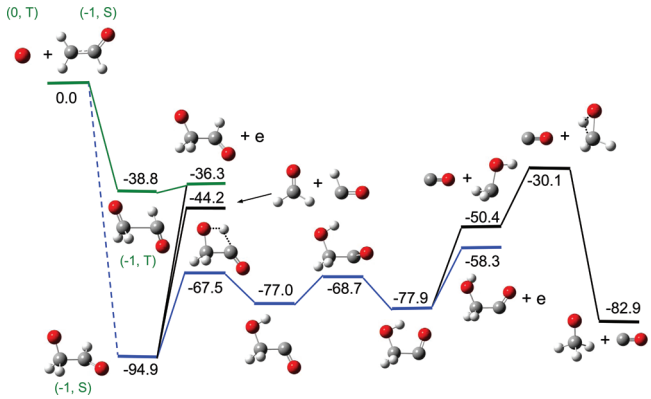

Figure 7. Reaction coordinate plot for CH_2CHO^- + O at 0 K. Calculations were performed at the (RO)MP2(full)/aug-cc-pVTZ//MP2(full)/aug-cc-pVDZ level of theory as described in the text. The number and letter in the parentheses indicate the charge and multiplicity for each state, respectively. The spin-allowed reaction is shown as the green line, the most dynamically favorable spin-forbidden channel is shown as the blue line, and other possible reaction channels are shown as black lines. The spin-conversion process is shown as dotted lines. The only ionic product is the associative product (OCH_2CHO^-), which is observed in trace amounts.

Similar experiments were also carried out for the reactions between O atoms and the larger nitrile anions, *i.e.*, CH_3CHCN^- and $(CH_3)_2CCN^-$; however, the complete reaction coordinate plots were not constructed. Instead, only the reaction enthalpies of the associative detachment and CN^- generation were calculated as summarized in Table 1. It is noted that all three systems have very high reaction efficiencies, indicating that they are collision-controlled processes. In general, these energetically accessible reaction pathways are more exothermic compared to the corresponding channels in the CH_2CN^- + O system. In addition, CN^- is a common ionic product observed from all three systems, whereas CCN^- is observed only in the reaction of O with CH_2CN^-. This result can be rationalized from the mechanisms of the corresponding reactions. As shown in Figure 5a, the formation of CN^- can occur through a spin-conserved process without an activation energy barrier. It is very likely that a similar reaction mechanism is involved in reactions of larger nitrile anions with O atoms. However, formation of CCN^- may proceed by different mechanisms. In the reaction of CH_2CN^- + O, the most favored pathway of CCN^- (triplet) formation involves two hydrogen transfer transition states that have no activation energy barriers relative to the triplet intermediate. In contrast, to form CCN^- from other nitrile anions, insertion of an O atom in the C−C bond and/or additional C−C bond cleavages seem to be necessary, such that higher energy transition states may be involved in the reactions. Thus, the formation of CCN^- may be energetically prohibited. The lack of CCN^- production does not have a pronounced effect on the overall efficiency of the reactions of CH_3CHCN^- and $(CH_3)_2CCN^-$ with O atoms, indicating that these reactions mainly proceed through the spin-conserved electron detachment and CN^- producing channels.

4.4. Reaction of CH_2CHO^- with O Atoms. As shown in Figure 7, the direct association of CH_2CHO^- with O atoms forms the triplet intermediate (−38.8 kcal/mol) that can undergo electron detachment, and the neutral product OCH_2CHO (doublet) is 36.3 kcal/mol below the total energy of the reactants:

$$^-CH_2CHO\ (S) + O\ (T) \rightarrow OCH_2CHO\ (D) + e^-, \quad \Delta H_0 = -36.3\ \text{kcal/mol} \qquad (11)$$

Similarly, the calculations indicate that the relative energy of the singlet−triplet crossing point is very close to that of the triplet state minimum (not shown), such that spin conversion may occur with a measurable rate during the approach of CH_2CHO^- with O atoms on the attractive potential energy curve; the energetically accessible reaction pathways are shown in Figure 7. The first pathway is the electron detachment from the singlet intermediate (−94.9 kcal/mol), and the neutral product is identical to that formed in reaction 11. The second pathway is the direct elimination of HCO^- via C−C bond cleavage from the singlet intermediate, and the third reaction channel involves two subchannels. In the third pathway, the singlet intermediate proceeds through two transition states and one intermediate to form an isomer, which can directly lose an electron to form the more stable isomer of neutral $HOCH_2CO$, or overcome additional energy barriers to produce CO and CH_3O^- products. The neutral product has a relative energy of −36.3 or −58.3 kcal/mol if the electron detachment occurs from the direct associative singlet intermediate or from one of the low energy isomers, respectively. Because the electron detachment from the singlet state isomer has the lowest activation energy barrier, it is likely to be the most favored channel among the singlet reaction pathways if spin conversion occurs. According to the experimental observations, the only ionic product is the association product (OCH_2CHO^-), which is observed in only trace amounts; therefore, electron detachment is facile for this reaction under our experimental conditions. Although it is not possible to determine whether the spin-allowed or spin-forbidden electron detachment channel is the major reaction pathway, it is reasonable that spin conversion is the rate-limiting step of the spin-forbidden reactions, such that the spin-conserved pathway is the major channel for this reaction.

5. Conclusions

The experimental and computational studies of CH_2CN^-, CH_3CHCN^-, $(CH_3)_2CCN^-$, and CH_2CHO^- reacting with N and O atoms were conducted to explore anion−atom reactions that may occur in interstellar clouds. The major ionic product of the reactions between nitrile anions (CH_2CN^-, CH_3CHCN^-, and $(CH_3)_2CCN^-$) and atoms (N and O) is CN^-, whereas CCN^- was also detected in the reaction of CH_2CN^- + O. In contrast, an ionic product was not observed for the reactions of CH_2CHO^- with N and O atoms, where electron detachment is a reasonable mechanism to deplete the CH_2CHO^- anion. The reactions of anions with O atoms exhibit larger reaction rate constants compared to the corresponding reactions with N atoms. This trend was investigated by theoretical computations, and the results indicate that the existence of energy barriers on the entrance channel of anions and N atoms are too high to be overcome by the reactants in the spin-conserved reactions. On the other hand, the relative energy of the doublet−quartet crossing point is fairly close to the total energy of the reactants on the entrance channel; spin conversion cannot occur with a sufficiently high rate, such that the efficiency of the reactions between anions and N atoms is rather low. In contrast, energy barriers do not exist in the reactions between anions and O atoms on the entrance channel, such that both spin-conserved and spin-forbidden reactions may be feasible, although the former processes will likely dominate. All the reactions of anions with O atoms exhibit very high efficiencies indicating they are essentially collision controlled processes. Our current results indicate that the major factor influencing the reaction efficiency

of anions with N and O atoms is whether spin-allowed barrierless reaction pathways exist. Although all experiments were performed under conditions of higher pressure and temperature than those that exist in the ISM, these reactions are two-body processes, such that the reaction rate constants are independent of pressure; moreover, temperature-variable experiments generally exhibit either a simple temperature dependence or no dependence. Therefore, laboratory measurements provide a valid approach to explore the ion chemistry of the ISM. Although spin-forbidden reactions exhibit low reaction efficiencies, they may still contribute in the ISM due to the extremely long time scales of clouds ($\sim 10^6$ years).[28] This work provides an understanding of the chemical mechanisms that may occur in the interstellar medium and allows us to explore some synthetic pathways that may lead to the formation and observation of large interstellar neutrals.

Acknowledgment. We gratefully acknowledge financial support from NASA, the NASA Graduate Student Researchers Program (GSRP), and the National Science Foundation (CHE-0647088). This research was supported in part by the National Science Foundation through TeraGrid resources provided by NCSA. We are grateful to Prof. Jeremy Harvey at Bristol University for providing the program to locate the crossing points between different spin states and for his helpful discussions. We thank Dr. Douglas J. Fox from Gaussian Company for his suggestions regarding the computations, Dr. Xuebin Wang at Washington State University for discussions, and Prof. John Tully at Yale University for his comments and suggestions.

Supporting Information Available: Complete ref 33. This material is available free of charge via the Internet at http://pubs.acs.org.

JA100673Z